Z. Phys. B 98, 187–195 (1995)

ZEITSCHRIFT
FÜR PHYSIK B

THz-field induced nonlinear transport and dc voltage generation in a semiconductor superlattice due to Bloch oscillations

Anatoly A. Ignatov[1,*], E. Schomburg[1], J. Grenzer[1], K.F. Renk[1], E.P. Dodin[2]

[1] Institut für Angewandte Physik, Universität Regensburg, Universitätstrasse 31, D-93040 Regensburg, Germany
[2] Institute for Physics of Microstructures, Russian Academy of Sciences, 603600 Nizhny Novgorod, Russia

Received: 23 November 1994/Revised version: 14 February 1995

Abstract. We report on a theoretical analysis of terahertz (THz-) field induced nonlinear dynamics of electrons in a semiconductor superlattice that are capable to perform Bloch oscillations. Our results suggest that for a strong THz-field a dc voltage should be generated. We have analyzed the real-time dynamics using a balance equation approach to describe the electron transport in a superlattice miniband. Taking account of both Bloch oscillations of electrons in a superlattice miniband and dissipation, we studied the influence of a strong THz-field on currently available superlattices at room temperature. We found that a THz-field can lead to a negative conductance resulting in turn in a THz-field induced dc voltage, and that the voltage per superlattice period should show, for varying amplitue of the THz-field, a form of twisted plateaus with the middle points being with high precision equal to the photon energy divided by the electron charge. We show that the THz-field can cause fast switching from the zero-voltage to the finite voltage state, and that in the finite voltage state dynamic localization of the electrons in a miniband occurs.

PACS: 73.20 Dx; 73.40 Gk

I. Introduction

On the basis of Bloch's description [1] of the motion of electrons in a periodic potential superimposed with a dc electric field, Zener showed [2] that Bloch oscillations can occur due to Bragg reflection of electrons. Esaki and Tsu [3] proposed to prepare superlattices of different semiconductor materials to realize a system that allows to observe Bloch oscillations. They also predicted [3] that the current-voltage characteristic of a superlattice should show a negative differential conductance if the Bloch oscillations are sufficiently weakly damped, namely, when electrons perform quasi-ballistic motion, with an average scattering frequency smaller than the Bloch frequency of the electrons.

Recently, Bloch oscillations have been observed in GaAs/GaAlAs superlattices, for free-electron motion along the superlattice axes. The occurrence of Bloch oscillations has been concluded from the observation of negative differential conductance [4–7], from studies of the decay of coherent nonequilibrium states prepared by interband transitions using femtosecond visible light pulses [8, 9], and by measuring the response to a THz-field [10]. The experiments demonstrate the possibility to observe fundamental quantum phenomena in tailored artificial crystals.

Various theoretical studies treated the influence of a strong high-frequency electric field (i.e. of a field with a frequency of the order of the Bloch frequency, assumed to be of the order of the scattering frequency) on the Bloch oscillations and the electron transport in superlattices. In particular, it has been shown [11, 12] that multiphoton absorption and emission processes can occur in the electronic system, resulting, under appropriate conditions, in a *negative conductance* $G = i_{dc}/V_{dc}$ of a superlattice where i_{dc} is the dc current flowing through the superlattice and V_{dc} the dc voltage across the superlattice; in case of a negative conductance ($G < 0$) the current flow is opposite to an applied dc electric field; see also Refs. [13–15]. The investigations [13–15] predict, moreover, that irradiation of a superlattice can result in a negative conductance at zero dc voltage and zero dc current with spontaneous switching of the system from an unstable state to a stable state that has a finite value of the dc voltage but zero dc current.

From a *quasi classical* treatment [13–15] it was predicted that spontaneous switching can occur when the high-frequency field causes a dynamic localization of the free electrons, and that the condition for dynamic localization is $J_0(eE_\omega a/\hbar\omega) \to 0$, where E_ω is the amplitude of a monochromatic ac field of frequency ω in the superlattice, a the superlattice period, $J_0(x)$ the Bessel function of zeroth order (e = elementary charge, $\hbar$ = Planck's constant). Under the condition of dynamic localization

* *Permanent address*: Institute for Physics of Microstructures, Russian Academy of Sciences, 603600 Nizhny Novgorod, Russia

the free-electron motion in a miniband is frozen in as a consequence of frequency modulation of the Bloch oscillations of the electrons by the ac field. Various *quantum mechanical* studies for ballistic electron motion in a superlattice miniband under the action of a strong driving ac electric field [16–22] have delivered the same criterion for dynamic localization. In both the quasi classical and the quantum mechanical studies [13–22] electron scattering has not been rigourously taken into account.

Theoretical studies of undamped [11] and weakly damped [12] Bloch oscillations suggest that under the condition of dynamic localization new stable states arise, characterized by dc voltages (over one superlattice period) that are multiples of $\hbar\omega/e$. The process resembles the inverse ac Josephson effect [23] in a stack of superconductor-insulator-superconductor hysteretic junctions [24]. It has been proposed to use a superlattice based frequency-to-voltage converter as a low temperature voltage standard [12]; it has been guessed [12] that electron scattering may result in dc voltage steps with values different from $\hbar\omega/e$.

In this paper we report on a study of quasiballistic electron motion in a superlattice along the superlattice axis. We treat the electrons as free particles in a superlattice miniband but suffering elastic and inelastic scattering. We apply a quasi classical balance-equation approach for describing the electron motion in the superlattice miniband [25] and assume an equivalent circuit, of a superlattice with a current source, that is similar to the equivalent circuit used in (small impedance) Josephson junction simulations [23]. Our calculations, performed for currently available superlattice diodes at room temperature [10, 26] will show that a current flowing through a superlattice created by an external THz-field, can generate a dc voltage, i.e. switching from a zero voltage to a finite voltage state, in case of quasi ballistic electron motion, and that electron scattering is even a necessary condition for switching. We will also show that the dependence of the ac field induced dc voltage on the amplitude of the external field has the form of twisted plateaus, with the middle point being with high precision equal to the photon energy divided by the electron charge ($\hbar\omega/e$).

We present results indicating that irradiation of currently available two-terminal superlattice devices at room temperature with strong THz-radiation should allow to observe dc voltage generation. We will furthermore discuss the response of a superlattice under strong radiation showing a complex scenario for the temporal variation of the voltage generation; universal behavior of the dc voltage generation is found for a large set of parameters. Our calculations deliver the dependence of the switching time on the THz-field strength; the switching time can be as short as few picoseconds. Finally, we will discuss dynamic localization taking account of electron scattering.

II. Principle of switching

We consider (Fig. 1a) a semiconductor superlattice consisting of N periods. Electrical contacts (one connected to ground) allow to apply an external THz-current $i_\omega^{ext}(t)$ and to measure the dc voltage across the superlattice; the

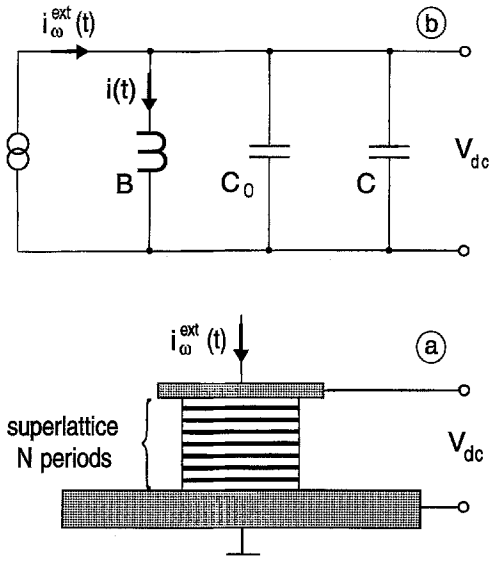

Fig. 1. a Superlattice switching: Under the influence of an external current $i_\omega^{ext}(t)$, a dc voltage across the superlattice V_{dc} is expected, and b, equivalent circuit; $i_\omega^{ext}(t)$ = external THz-current, B = superlattice capable to perform Bloch oscillations, C_0 = superlattice capacitance, C = parasitic capacitance, V_{dc} = dc voltage across the superlattice, $i(t)$ = electric current through the superlattice

current may be created by focusing THz-radiation on an antenna wire connected to the superlattice [10]. At an appropriate strength of the THz-field that is induced in the superlattice by the THz-current, a dc voltage V_{dc} may be expected; from theoretical studies neglecting scattering of electrons in the superlattice $V_{dc} = \pm N\hbar\omega/e$ has been suggested [11, 12].

We will calculate the voltage response of the superlattice using an equivalent circuit description (Fig. 1b), with a THz-current source delivering the external current $i_\omega^{ext}(t)$ of frequency ω, the time-dependent current $i(t)$ through the superlattice (B) that contains electrons capable to perform Bloch oscillations, the superlattice capacitance $C_0 = \eta S(4\pi L)^{-1}$, where η is the (average) dielectric constant of the superlattice material, S the superlattice area, L the length of the superlattice (L = Na, a = superlattice period), and C a parasitic capacitance in parallel to the superlattice capacitance.

The equivalent circuit corresponds to a circuit used for Josephson junctions [23]. However, there is a severe difference: While in a Josephson junction no losses due to scattering of the current-carrying carriers (Cooper pairs) occur, there is dissipation in the superlattice (B in Fig. 1 b) due to electron scattering.

III. Equations for the superlattice dynamics

For a description of the superlattice dynamics we use, following [3], a quasi classical description of the electron transport, with a quantum mechanical energy dispersion relation, a wave packet description of the electron motion and the (classical) Boltzmann equation for the electron distribution function. We consider the energy spectrum of

electrons in a miniband of the superlattice in a tight-binding approximation

$$\varepsilon(p) = \frac{1}{2}\Delta[1 - \cos pa/\hbar] \tag{1}$$

where ε is the kinetic energy, p the quasi momentum of an electron along the superlattice axis (perpendicular to the layers), Δ the miniband width, and a the superlattice period.

The quasi classical velocity $v(p)$ of an electron moving along the superlattice axis is given by the expression

$$v(p) = \frac{\partial\varepsilon(p)}{\partial p} = \frac{\Delta a}{2\hbar}\sin\frac{pa}{\hbar} \tag{2}$$

showing that the velocity of electrons in a miniband is a periodic function of the momentum, with maximum velocity $\frac{1}{2}\Delta a/\hbar$. The macroscopic-average state of electrons in the superlattice miniband may be specified by the time dependent distribution function $f(p, t)$ satisfying the Boltzmann equation

$$\frac{\partial f}{\partial t} + eE(t)\frac{\partial f}{\partial p} = St(f) \tag{3}$$

where $E(t)$ is the time dependent electric field directed along the superlattice axis and $St(f)$ the collision integral.

In order to take into account both elastic and inelastic lattice scattering of electrons we introduce a collision integral of the form [25]

$$St(f) = -\nu_\varepsilon[f(p, t) - f_0(p)] - \tfrac{1}{2}\nu_{el}[f(p, t) - f(-p, t)] \tag{4}$$

where $f_0(p) = \frac{1}{2}a[\pi\hbar I_0(\Delta/2kT)]^{-1}\exp[(2kT)^{-1}\Delta\cos pa/\hbar]$ is the equilibrium distribution function, T the lattice temperature, ν_ε an average energy-relaxation frequency, ν_{el} an average frequency of elastic collisions, and $I_n(x)$ the modified Bessel function of nth order.

The average electron velocity $V(t)$ and average electron energy $\mathscr{E}(t)$ are, respectively,

$$V(t) = \int v(p)f(p, t)\mathrm{d}p \tag{5}$$

$$\mathscr{E}(t) = \int \varepsilon(p)f(p, t)\mathrm{d}p \tag{6}$$

where the integration is carried out within the Brillouin zone, $-\pi\hbar/a < p \leq \pi\hbar/a$. Both $f(p, t)$ and $f_0(p)$ satisfy normalization conditions, $\int f(p, t)\mathrm{d}p = 1$ and $\int f_0(p)\mathrm{d}p = 1$.

The electron current density j along the superlattice axis is given by the general equation

$$j = neV \tag{7}$$

where n is the density of electrons in the superlattice miniband assumed to be spatially uniform. Instead of solving the set of (3) to (6), we derive the balance equations as ordinary differential equations for $V(t)$ and $\mathscr{E}(t)$. Multiplying (3) by $v(p)$ and $\varepsilon(p)$, respectively, and integrating over the Brillouin zone in momentum space we obtain

$$\frac{\partial V}{\partial t} + eE\int v(p)\frac{\partial f}{\partial p}\mathrm{d}p = -\nu_V V \tag{8}$$

$$\frac{\partial \mathscr{E}}{\partial t} + eE\int \varepsilon(p)\frac{\partial f}{\partial p}\mathrm{d}p = -\nu_\varepsilon(\mathscr{E} - \mathscr{E}_T) \tag{9}$$

where $\mathscr{E}_T = \frac{1}{2}\Delta(1 - \mu)$ is the mean thermal electron energy that corresponds to the velocity component along the superlattice axis, $\nu_V = \nu_\varepsilon + \nu_{el}$ the relaxation frequency of the average velocity, and $\mu = I_1(\Delta/2kT)/I_0(\Delta/2kT)$. Making use the relations

$$\frac{\partial v(p)}{\partial p} = \frac{\Delta a^2}{2\hbar^2}\left(1 - \frac{2\varepsilon(p)}{\Delta}\right) \tag{10}$$

$$\frac{\partial\varepsilon}{\partial p} = v(p) \tag{11}$$

and taking account of the periodicity of the distribution function $f(p, t)$ in the momentum space we calculate the integrals involved in (8) and (9) by parts and obtain

$$\dot{V} = eE/m(\mathscr{E}) - \nu_V V \tag{12}$$

$$\dot{\mathscr{E}} = eEV - \nu_\varepsilon(\mathscr{E} - \mathscr{E}_T) \tag{13}$$

where $m(\mathscr{E}) = m_0(1 - 2\mathscr{E}/\Delta)^{-1}$ is the energy dependent effective mass of the electrons in the superlattice miniband and $m_0 = 2\hbar^2/\Delta a^2$ the effective mass at the bottom of the miniband.

Equation (12), describing the dynamics of the "average electron" in a superlattice miniband, can be considered as Newton's law for the motion of the electron, with energy-dependent mass $m(\mathscr{E})$, while (13) represents the energy conservation law. When energy and velocity relaxation are neglected ($\nu_\varepsilon, \nu_V \to 0$) the balance equations (12) and (13) can be directly derived from (1) and (2), using the acceleration theorem [1, 2]

$$\dot{p} = eE(t) \tag{14}$$

that describes dissipationless (ballistic) electron motion. Accordingly, (12) and (13) describe in a simple way quasiballistic propagation of electrons in a miniband, with acceleration by an electric field and suffering friction.

To calculate the superlattice response to a high-frequency electric field we make use of the equivalent circuit of Fig. 1 b. The current through the superlattice $i(t)$ and the voltage $u(t)$ across the superlattice are governed by the equation

$$(C + C_0)\,\dot{u}(t) + i(t) = i^{\mathrm{ext}}(t) \tag{15}$$

where $i(t) = j(t)\,S$.

We introduce dimensionless variables, $\tau = \omega t$ for the time, $U(\tau) = eE(t)\,a(\hbar\omega)^{-1}$ for the voltage drop per one superlattice period, $I(\tau) = 2\hbar(Se n\Delta\mu a)^{-1} i(t)$ for the current, $I^{\mathrm{ext}}(\tau) = 2\hbar(Se n\Delta\mu a)^{-1} i^{\mathrm{ext}}(t)$ for the external current, and the difference W, between the average electron energy and the mean thermal energy, $W = 2(\mathscr{E} - \mathscr{E}_T)(\Delta\mu)^{-1}$. We find from (12), (13) and (15) the following set of nonlinear ordinary differential equations

$$\dot{I} = U(1 - W) - \nu_I I \tag{16}$$

$$\dot{W} = UI - \nu_W W \tag{17}$$

$$C_{\mathrm{eff}}\dot{U} = I^{\mathrm{ext}}(\tau) - I \tag{18}$$

describing nonlinear transport in an irradiated semiconductor superlattice two terminal device. The equations contain only three (dimensionless) parameters, namely the (dimensionless) velocity-relaxation frequency $\nu_I = \nu_V/\omega$,

the energy-relaxation frequency $\nu_W = \nu_\varepsilon/\omega$ and the effective capacity $C_{eff} = \omega^2(1 + C/C_0)/\omega_0^2\mu$ where $\omega_0 = (4\pi e^2 n/\eta m_0)^{1/2}$ is the plasma frequency.

We derived (16)- (18) with a quasi one-dimensional model for the collision integral, with the relaxation frequencies ν_I and ν_W; these can be considered as phenomonological parameters which can be extracted from either measured or simulated data for the static current-voltage characteristic.

In the two-relaxation frequency model, a steady state solution of (16)–(18) gives the static current-voltage characteristic in a form [25] $I = U\nu_I^{-1}[1 + U^2/\nu_I\nu_W]^{-1}$. The current has a peak value $I_p = \frac{1}{2}\delta^{1/2}$ where $\delta = \nu_W/\nu_I$ ($\delta \leq 1$) at the critical voltage $U_c = (\nu_I\nu_W)^{1/2}$. In the special case that we ignore elastic scattering we have $\nu_W = \nu_I = \nu$, where $\nu = \nu_S/\omega$ is the characteristic scattering frequency in dimensionless units, and $\nu_S = \nu_\varepsilon = \nu_V$. We then find for the current-voltage characteristic the Esaki-Tsu formula [3], with $I_p = \frac{1}{2}$ and $U_c = \nu$. In our treatment the factor δ describes, for $\delta < 1$, the effect of carrier heating yielding to a suppression of the peak current I_p below the value $I_p = \frac{1}{2}$ [25]. This effect has recently been carefully studied by dc measurements of the current-voltage characteristic of superlattices [4] that gave $\delta \approx 0.2$ and by time-of-flight experiments [27], where $\delta \approx 0.1$ was found. The effect (with $\delta \approx 0.03$) was also revealed by comparison of simulations [28] with experiments [29, 30] on multistability effects in semiconductor superlattices caused by a negative differential conductivity. Of course, the value of δ depends on the specific parameters of a sample and its lattice temperature.

IV. Photon-assisted dc transport

We will now show, how electron transitions with multiphoton emission and absorption are incorporated in our nonlinear equations. We discuss the case of an external ac current of frequency ω, with ω being high enough so that $C_{eff} \gg 1$. Then, the displacement current is large compared to the electron current and (18) describes the establishment of a monochromatic ac voltage with the amplitude $U_\omega = I_\omega^{ext}/C_{eff}$ per superlattice period.

We now suppose that, in addition to the oscillating voltage, a slowly varying voltage U_0 appears and that the total voltage is

$$U(\tau) = U_0 + U_\omega \cos(\tau + \varphi) \tag{19}$$

where ϕ is the phase shift between the voltage and the external current. By time averaging of (18) over a period of the external current, we find the relation

$$C_{eff}\frac{dU_0}{d\tau} = I_0^{ext} - I_0(U_0, U_\omega) \tag{20}$$

where I_0^{ext} is an external dc current flowing in addition to the high-frequency external current and where

$$I_0(U_0, U_\omega) = 1/2\pi \int_{2\pi} I(\tau, U_0, U_\omega)d\tau \tag{21}$$

describes the static current-voltage characteristic of the superlattice in the presence of an ac voltage, and $I(\tau, U_0, U_\omega)$ is the solution of (16) and (17).

Supposing that the time of irradiation of a superlattice (laser pulse duration) is much longer than the characteristic scattering times, we find a solution of (16) and (17) for an arbitrary periodic function $U(t)$ in the form

$$I(\tau) = \int_{-\infty}^{\tau} \nu d\tau_1 e^{-\nu(\tau-\tau_1)} \sin\left[\int_{\tau_1}^{\tau} U(\tau_2)d\tau_2\right] \tag{22}$$

$$W(\tau) = 1 - \int_{-\infty}^{\tau} \nu d\tau_1 e^{-\nu(\tau-\tau_1)} \cos\left[\int_{\tau_1}^{\tau} U(\tau_2)d\tau_2\right] \tag{23}$$

where we used, for simplicity, a single relaxation frequency approximation, $\nu_I = \nu_W = \nu$. The solutions given by (22) and (23) do not depend on the initial conditions for I and W, because scattering completely destroys the coherence of electron motion in time intervals longer than the inverse scattering frequency ν^{-1}.

In case of a monochromatic driving voltage the time averaging of (22) yields [13]

$$I_0(U_0, U_\omega) = \int_0^{\infty} \nu d\tau\ e^{-\nu\tau} \sin(U_0\tau)\ J_0(2U_\omega \sin\tau/2) \tag{24}$$

where $J_0(x)$ is the Bessel function of zeroth order. The last equation has the same form as the equation describing current flow in a superlattice miniband, with electrons performing Bloch oscillations with the Bloch frequency $\Omega_B = eE_0a/\hbar$ and suffering scattering [3], except of the factor $J_0(2U_\omega \sin\tau/2)$, which implies frequency modulation of the Bloch oscillations by the external ac field.

Using the Fourier expansion

$$J_0(2U_\omega \sin\tau/2) = J_0^2(U_\omega) + 2\sum_{n=1}^{\infty} J_n^2(U_\omega)\cos n\tau \tag{25}$$

we find for the static current-voltage characteristic of an irradiated superlattice

$$I_0(U_0, U_\omega) = \sum_{n=-\infty}^{\infty} J_n^2(U_\omega)\ I_0^{ET}(U_0 + n) \tag{26}$$

where $I_0^{ET} = U_0\nu^{-1}[1 + (U_0/\nu)^2]^{-1}$ is the Esaki-Tsu current-voltage characteristic [3].

Thus, we see that an ac electric field (voltage) produces new channels for dc current flow in a superlattice, due to multiphoton absorption or emission. The probability of absorbing (or emitting) n photons is given by $J_n^2(U_\omega)$ and the resulting current-voltage characteristic corresponds to the Esaki-Tsu characteristic weighted with $J_n^2(U_\omega)$ and shifted by $n\hbar\omega/e$ in the scale E_0a, which is the dc voltage drop per superlattice period. For $\nu \to 0$ the current-voltage characteristic looks like a set of vertical spikes similar to that given in [11], with negative conductance, i.e. current flow against the applied dc electric field, which is due to absorption of photons.

It follows from (26) that without photon emission or absorption the current I_0 is zero if $J_0(U_\omega) = 0$, i.e. there is no electron motion without photon emission or absorption. This is the case of dynamic localization of the electrons in the miniband due to frequency modulation of the Bloch oscillations by the external field.

Under the condition of dynamic localization photon absorption and emission processes, $J_n^2(U_\omega) \neq 0$, cause finite dc current flow, resulting in a negative conductance near the zero-voltage/zero-current state. This state is therefore unstable, and switching occurs spontaneously to a finite-voltage state, which can be described by (20).

Examples of current-voltage characteristics calculated from (26) are drawn in Fig. 2. For an ac frequency smaller than the scattering frequency ($\omega/\nu_S < 1$, upper part of the figure) the current-voltage characteristic corresponds to the Esaki-Tsu characteristic (for $U_\omega \ll 1$) or is modified under the influence of an ac field ($U_\omega = 1$ and $U_\omega = 2.4$); the ac field amplitude $U_\omega = 1$ corresponds to a field amplitude (E_ω) at which an electron can gain or loose, per superlattice period, the quantum energy $\hbar\omega$. In all cases a negative differential conductance occurs at large values of the dimensionless dc voltage U_0; for $U_0 = 1$ the energy eE_0a an electron gains per superlattice period the quantum energy $\hbar\omega$ of the external dc field. For a frequency larger than the scattering frequency (curves in the middle of the figure, $\omega/\nu_S = 2$) a negative conductance occurs at large ac field values ($U_\omega = 2.4$). In this case the zero-voltage/zero-current state is unstable, i.e. the system will switch to a finite voltage state. If there is no dc current flow, the corresponding voltage is near $U_0 = 1$, i.e. that the dc voltage drop per superlattice period (E_0a) is close to $\hbar\omega/e$; in spite of strong scattering ($\omega/\nu_S = 2$) the value of the voltage drop we expect is near the value calculated for the case $\nu = 0$. For the case of weak scattering ($\omega/\nu_S = 5$, lower curves) the negative-conductance state at zero voltage is expected to switch to a voltage state with U_0 of almost 1.

Currently available superlattices have, at room temperature, a characteristic scattering frequency $\nu_S \approx 10^{13}$ s^{-1} [25]. We therefore suggest that a state of negative conductance can be created in a superlattice at room temperature by use of a THz-field ($\omega > 10^{13}$ Hz) and, that application of a THz-field to a superlattice (at room temperature) can lead to switching from zero dc voltage to a finite dc voltage state, with a dc voltage drop per superlattice period of about $\hbar\omega/e$.

We have calculated, using (26), the dependence of the dc conductivity on the strength of the ac voltage (Fig. 3). For strong scattering ($\omega/\nu_S < 1$) the dc conductivity is positive; with increasing strength of the ac field the dc conductivity decreases (upper curves). In case of weak scattering ($\omega/\nu_S > 1$) the dc conductivity decreases strongly with U_ω and then oscillates around $\sigma_{dc} = 0$, with intervals of negative conductivity. The width of these intervals is largest for $\omega/\nu_S \sim 2$ and decreases for increasing ω/ν_S.

In the limiting case of strong scattering ($\omega \ll \nu_S$) we find from (26), for $U_0 \to 0$, the approximation

$$\sigma_{dc}(U_\omega)/\sigma_0 = \frac{1}{[1 + (U_\omega/\nu)^2]^{3/2}} \tag{27}$$

which shows that the dc conductivity decreases for $U_\omega \ll \nu$ as $\sigma_{dc}/\sigma_0 \approx 1 - \frac{3}{2}(ea/\hbar\nu_S))^2 E_\omega^2$. The reduction of conductivity increases quadratically with the ac field strength. This is the basis for the use of a superlattice device as power detector for millimeter wave radiation (this will be published separately). For a large ac field strength, $U_\omega \gg \nu$, the dc conductivity decreases strongly, $\sigma_{dc}/\sigma_0 = (\hbar\nu_S/ea)^3 E_\omega^{-3}$. At high field strength the conductivity of the superlattice is strongly suppressed.

We can obtain an analytical expression for the dc conductivity of the irradiated superlattice for the case of negligible scattering ($\nu \to 0$). We find, with $U_0 \lesssim \nu$, from (26) an approximate expression for the current (in the limit $\nu \to 0$)

$$I_0(U_0, U_\omega) = J_0^2(U_\omega) \frac{U_0}{\nu[1 + (U_0/\nu)^2]} \tag{28}$$

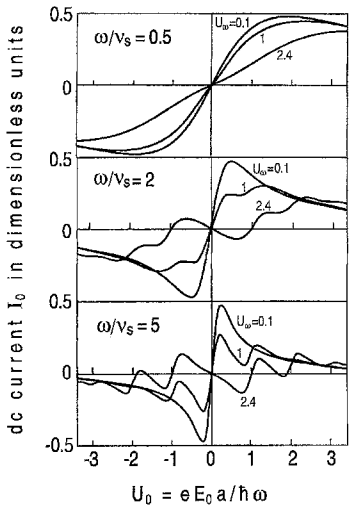

Fig. 2. Current-voltage characteristics of a superlattice in the presence of a strong ac field calculated analytically from (26) for strong scattering (upper curves) and weaker scattering (middle and lower curves) for a weak ac field ($U_\omega = 0.1$), a strong ac field ($U_\omega = 1$) and a very strong ac field ($U_\omega = 2.4$); ω = frequency of the ac-field, ν_S = average scattering frequency, $U_\omega = eE_\omega a/\hbar\omega$ = ac voltage amplitude

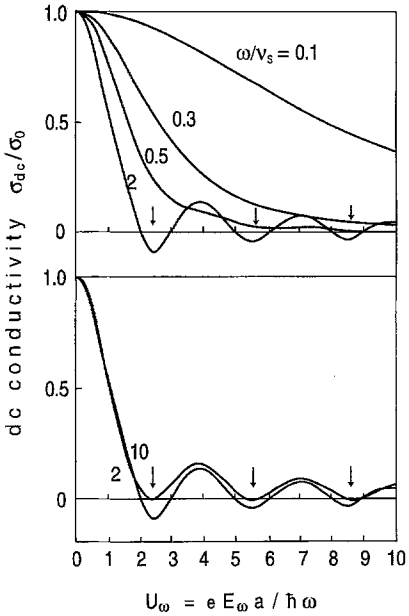

Fig. 3. Dc conductivity of a superlattice plotted as a function of the ac voltage amplitude U_ω for different strengths of scattering (ω = frequency of the ac field, ν_S = scattering frequency). The arrows indicate regions of negative conductivity

which shows that in the limit of negligible scattering photon processes (with $n = \pm 1, \pm 2 \ldots$) do not contribute to the dc transport and that the dc Esaki-Tsu current-voltage characteristic is multiplied by $J_0^2(U_\omega)$. Consequently, we obtain

$$\sigma_{dc}(U_\omega)/\sigma_0 = J_0^2(U_\omega) \tag{29}$$

which corresponds to a conductivity that is equal to the conductivity without ac field multiplied by $J_0^2(U_\omega)$. It follows that in the limit $v \to 0$ a negative conductivity does not occur, i.e. that without dissipation the zero-voltage/zero-current state is stable.

In case of $v \neq 0$ this state is unstable and switching occurs to a finite voltage state, with not completely negligible current (because of consumption of energy in the voltage measuring device). The energy for switching and for maintaining the stable state is delivered by the external ac field, with the electrons performing multiphoton ($n = \pm 1, \pm 2, \ldots$) transitions.

We can calculate the time of switching from the unstable state ($U_0 = 0$) to the stable state ($U_0 \simeq 1$). Using a piecewise approximation of the function $I_0(U_0, U_\omega)$ by straight lines we find from (20) and (26) for the switching time (in dimensionless units), τ_{SW}, the approximate expression

$$\tau_{SW} = \frac{2C_{\text{eff}} \nu_I \ln|\frac{1}{2}(\delta U)^{-1}|}{|\sigma_{dc}(U_\omega)\ |\sigma_0^{-1}} \tag{30}$$

where $\sigma_{dc}(U_\omega)$ is the small dc field ($U_0 \to 0$) negative conductivity in the presence of a strong ac driving voltage U_ω, σ_0 the dc conductivity at small U_0 and $U_\omega = 0$, and δU the amplitude of an initial perturbation of the system. The switching time is proportional to the capacity C_{eff} and to the velocity relaxation frequency ν_I, and decreases with increasing perturbation. The switching time is very large for small negative values of the conductivity, $\sigma_{dc}(U_\omega) \approx 0$, and reaches the smallest values for large (negative) values of $\sigma_{dc}(U_\omega)$. The shortest switching time is expected for values $v \sim 2$ to 5 (see Fig. 3).

V. Circuit dynamics

The idea of photon-assisted transport delivers a key for an understanding of the complex nonlinear dynamics of the ac current driven superlattice, described by (16)–(18).

Let us analyze the case when a THz-current, adiabatically switched on, drives the superlattice according to

$$I^{\text{ext}}(\tau) = I_\omega^{\text{ext}}[1 - \exp(-\tau/\tau_0)]\cos\tau \tag{31}$$

where τ_0 is the time of switching-on of the THz-current. In this case the time dependent current $I(\tau)$ and voltage $U(\tau)$ can be obtained as numerical solutions of (16)–(18). We use the conditions $I(\tau = 0) = 0, W(\tau = 0) = 0$, and $U(\tau = 0) = 0.005$ for an initial spontaneous perturbation of the system.

As an example, we consider a GaAs/AlAs superlattice at $T = 300$ K with the miniband width $\Delta = 110$ meV ($\mu \approx 0.72$), for THz-radiation delivered by a far-infrared laser emitting radiation of a wavelength of 118 μm ($\omega = 1.6 \cdot 10^{13} s^{-1}$), and scattering frequencies

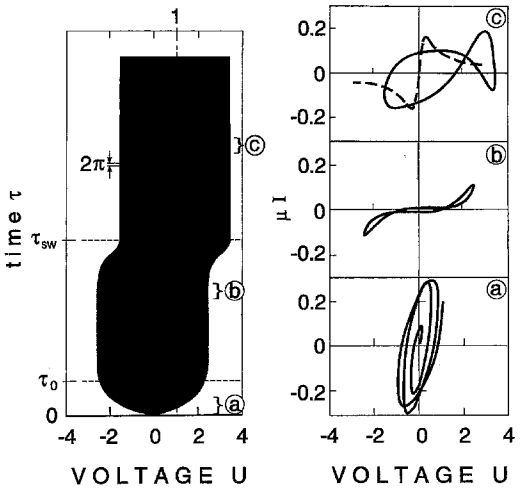

Fig. 4. Calculated voltage U across a superlattice period as a function of the dimensionless time, $\tau = \omega t$. The period of oscillation (2π) is small in the time scale and not resolved in the figure. Current-voltage phase-plane diagrams corresponding to three different modes of operation are indicated on the right side of the figure (I = current in normalized units, $\mu = I_1/I_0$): (a), transient process; (b), unstable limit cycle; (c), stable limit cycle, with time averaged voltage $V_{dc}^1 = \hbar\omega/e$; the dashed curve shows the static current-voltage characteristic used in the simulations

$\nu_V = 1.1 \cdot 10^{13} s^{-1}$, $\nu_\varepsilon = 2.2 \cdot 10^{12} s^{-1}$ ($\nu_I = 0.69$, $\nu_W = 0.14$, $\delta = 0.2$) extracted from experimental static current-voltage characteristics [25]. For typical carrier densities in a superlattice, $n \approx 10^{16} - 10^{17}$ cm^{-3}, the parameter μC_{eff} lies in the range $0.7 \gtrsim \mu C_{\text{eff}} \lesssim 7$. We choose $\mu C_{\text{eff}} = 1$ and 3 for simulations.

Figure 4. shows, for $I_\omega^{\text{ext}}/C_{\text{eff}} = 2.4$, the dynamics of the switching. During switching-on of an external THz-current within the time τ_0 an ac voltage U across the superlattice develops, having a mean value $\bar{U} \approx 0$ (left part of Fig. 4). At the switching time τ_{SW} the system jumps to a state with a mean voltage near $\bar{U} = 1$. On the right side of Fig. 4 we show in the current-voltage space for three different time intervals instantaneous values of current and voltage. The interval (a) corresponds to the transient response of the system during the start of the external field, with increasing external current amplitude across the superlattice. In the interval (b) the system is in a quasi anti-symmetrical unstable current-voltage limit cycle with slow drift of the time averaged voltage towards the positive direction initiated by the external perturbation $U(\tau = 0) > 0$. Then, a rapid flop occurs to the stable limit cycle. The time interval (c) characterizes the stable state with the time averaged voltage close to $\hbar\omega/e$, i.e. $\bar{U} = \int_{2\pi} U(\tau)\mathrm{d}\tau = 1$.

VI. Results of the simulations

In Fig. 5 we summarize the results of simulations. First we show, Fig. 5a, the dependence of the dc conductivity on the amplitude of the ac voltage U_ω obtained by solving (16) and (17) for a small constant voltage $U_0 \ll 1$ (at increasing ac voltage) with a small current flowing in addition to an ac current; current flow is, e.g., possible

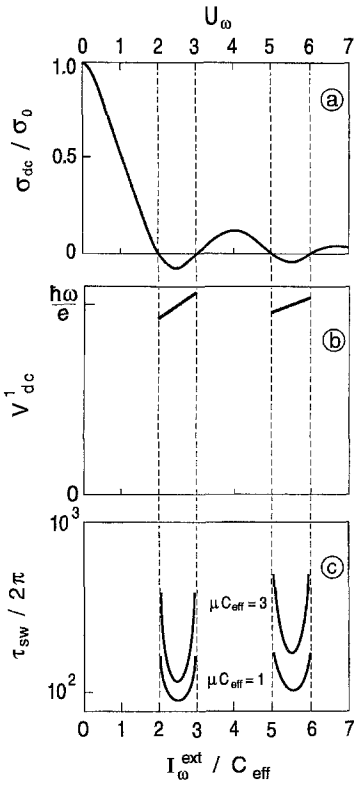

Fig. 5. **a** dc conductivity as a function of the ac voltage amplitude $U_\omega = eE_\omega a/\hbar\omega$ and **b** dc voltage per one period V_{dc}^1 as function of the external-current amplitude I_ω^{ext}/C_{eff}; **c**, switching time for two values of the effective device capacitance μC_{eff}.

through the voltage measuring device. As expected, we find negative values of the conductivity in regions near the points of dynamic localization, where $J_0^2(U_\omega) \to 0$. Results obtained by direct numerical simulation of the total system decribed by (16)–(18) are drawn in Fig. 5b and c, showing the instability regions in the I_ω^{ext}/C_{eff} scale. Figure 5b shows the dc (time averaged) voltage per one period, $V_{dc}^{(1)}$, expected for a superlattice at appropriate irradiation. The dependence of the dc voltage on the strength of the ac current has a form of twisted plateaus, with the middle points being, within an accuracy of the numerical calculations, equal to $\hbar\omega/e$. In Fig. 5 (c) we have drawn the dependence of the switching time ($\tau_{SW}/2\pi$) counted in number of periods of the ac current. The time is in good agreement with the analytical formula of (30); for $\sigma_{dc}(U_\omega)/\sigma_0$ we used the data of Fig. 5 (a) and the initial condition $U(\tau = 0) = 0.005$. The switching time strongly depends on C_{eff} while the voltage $V_{dc}^{(1)}$ is, for our parameters and within the accuracy of our calculations, independent of C_{eff}, i.e. $V_{dc}^{(1)}$ does not depend on the switching time. We find a switching that is fastest at the largest value of the negative conductivity and is of the order of a picosecond.

We would like to mention that electron transport in a superlattice can be described within the framework of a Bloch type quasiclassical model as presented in this paper, if the voltage drop per one period is smaller than a superlattice miniband width, i.e. $eEa < \Delta$. Then, the spatial amplitudes of electron trajectories $X \approx \Delta/eE$ are larger than the superlattice period [31]. This condition implies that $U < \Delta/\hbar\omega$ and, for our special example, $U < 11$. As one can see from Fig. 4 this condition is well satisfied.

In order to observe dc voltage creation by a THz-field, the required field strength follows from the condition $J_0(U_\omega^*) \lessgtr 0$. Fastest switching (for the first band of instability) occurs for $U_\omega^* \approx 2.4$. Then the amplitude of the ac voltage across the superlattice is $V_{ac} \approx 2.4 \cdot N\hbar\omega/e$, and for $\omega \approx 1.57 \cdot 10^{13} s^{-1}$ and $N \approx 50$, $V_{ac} \approx 0.5$ V. The ac power P_{ac} dissipated in the superlattice is $P_{ac} = \frac{1}{2} V_{ac}^2 R_{ac}$, where R_{ac} is the ac resistance. For a typical superlattice device [10] a resistance at THz-frequencies of $R_{ac} \approx 100\Omega$ can be achieved for a diameter of a superlattice $D \approx 5\mu$m. Then, $P_{ac} \approx 1.3$ mW. This power level (4 kW/cm^2) in the superlattice is readily achievable with currently available far-infrared lasers, even at a low efficiency of antennas for THz-radiation [10].

VII. Dynamic localization

Recent quantum mechanical treatments of electron states in a superlattice in a time dependent field [16–22] have shown that the superlattice miniband width becomes zero under the condition of dynamic localization, $J_0(eE_\omega a/\hbar\omega) = 0$. This "miniband collapse" [18] has been attributed to an interplay of the spatial periodicity of the superlattice potential and the temporal periodicity of the external ac field in the Schrödinger equation. We now will show how this effect is involved in our quasiclassical treatment of the superlattice response and discuss its relation to dc transport in a superlattice irradiated with THz-radiation.

We discuss the case of ballistic electron motion, i.e. we neglect scattering ($\nu_I = \nu_W \equiv 0$). We obtain from (16) and (17) the solutions

$$I = \sin\left\{\int_0^\tau U(\tau_1)\mathrm{d}\tau_1 + \varphi_0\right\} \tag{32}$$

$$W = 1 - \cos\left\{\int_0^\tau U(\tau_1)\mathrm{d}\tau_1 + \varphi_0\right\} \tag{33}$$

describing coherent motion of ballistic (unscattered) electrons in a superlattice miniband with the initial condition $I(\tau = 0) = \sin\varphi_0$ for the current, $W(\tau = 0) = 1 - \cos\varphi_0$ for the energy, and φ_0 for the momentum (in dimensionless units).

We introduce the integral $x(t) = \int_0^t v(t_1)\mathrm{d}t_1 + x_0$ for characterizing the motion of an electron in real space. Then, for a monochromatic ac field superimposed to a dc field, (32) gives the following solution for the electron trajectory

$$x(t) = v_0 \sum_{n=-\infty}^{\infty} J_n\left(\frac{eE_\omega a}{\hbar\omega}\right) \frac{1}{\omega_B + n\omega} \{\cos\varphi_0 - \cos[(\omega_B + n\omega)\, t + \varphi_0]\} + x_0 \tag{34}$$

where $v_0 = \frac{1}{2}\Delta a/\hbar$ is the peak velocity, $\omega_B = eE_0 a/\hbar$ the Bloch frequency of the electron oscillation in a constant dc field of amplitude E_0, and E_ω and ω are the amplitude and frequency of the external ac field, respectively.

Equation (34) decribes the electron localization in real space, namely, without multiphoton transitions the amplitude of x becomes zero for $J_0 = 0$, i.e. the electrons are completely spatially localized. At large frequency of the ac field, $\omega \gg \omega_B$ (with $\varphi_0 = 0$, and $x_0 = 0$ at $t = 0$), (34) becomes

$$x(t) = \frac{1}{2} X_0 J_0\left(\frac{eE_\omega a}{\hbar\omega}\right)(1 - \cos\omega_B t) \tag{35}$$

where $X_0 = \Delta/eE_0$ is the spatial amplitude of Bloch oscillations in the absence of an ac driving field. It follows from (35) that in the high-frequency limit ($\omega \gg \omega_B$) the effect of an ac field on a ballistic electron oscillating with the Bloch frequency ω_B in a superlattice leads to a dramatic reduction of the spatial amplitude X_0. The effect can be taken into account by simple renormalization of the "collapsing" superlattice miniband width $\Delta \to \Delta J_0(eE_\omega a/\hbar\omega) \to 0$, in agreement with the results of quantum mechanical treatments [16–22].

One might intuitively suggest that the same renormalization could be valid for the dc transport in a superlattice in an applied THz-field, with the dc conductivity proportional to Δ, according to $\sigma_{dc} = en/m_0\nu_S$, where ν_S is the characteristic scattering frequency and $m_0 = 2\hbar^2/\Delta a^2$ the effective mass of carriers at the miniband bottom, which would lead to $\sigma_{dc} \sim \Delta$. However, for the limiting case $\omega \gg \nu_S$, (29) delivers a quadratic dependence on J_0, $\sigma_{dc} \sim J_0^2(eE_\omega a/\hbar\omega)$. This difference indicates that electron scattering plays an essential role in the THz-response even if $\omega \gg \nu_S$. Our results indicate that in the limit of extremely weak scattering the dc conductivity shows an almost negligible range of negative conductivity, i.e. switching from the zero-voltage/zero-current state takes, according to (30), an almost infinite time of switching. Assuming that the time of irradiation (laser pulse duration) is much longer than the inverse scattering frequency ν_S^{-1}, (32) and (33) describing the dynamics of ballistic (unscattered) electrons in a miniband are no longer valid and one should use (22) and (23), or the basic (16) and (17), in order to take into account scattering. Our analysis shows that under the influence of a high-frequency field ($\omega \gg \omega_B$ and $\omega/\nu_S \gg 1$) an electron performs in the average a quasiballistic motion, with ballistic motion over ω/ν_S periods.

In case of stronger scattering irradiation of a superlattice with a strong THz-field ($\omega > \nu_S$) leads to fast switching as we have shown. The stable state, with a THz-field induced dc voltage, is associated with dynamic localization of the electrons in the superlattice miniband.

We would like to mention that in a recent paper [32] a theoretical investigation of terahertz emission and four-wave-mixing due to a quantum mechanical treatment of damped Bloch oscillations has been presented. The method [32] should, in principle, also allow to analyze the THz-field induced nonlinear transport in a semiconductor superlattice.

VIII. Conclusion

In conclusion, using a balance equation approach we have derived a set of nonlinear equations describing high-frequency properties of electrons in a semiconductor superlattice in a strong high-frequency electric field. Our real-time simulations performed for currently available superlattices at room temperature exposed to a strong THz-field have revealed the possibility of fast spontaneous generation of a dc voltage due to an instability caused by a negative conductivity due to carriers in a miniband that are capable to perform Bloch oscillations. We have found that the dependence of the dc voltage per one superlattice period on the ac driving current amplitude is expected to have a form of twisted plateaus, with the middle points being equal to the photon energy divided by the electron charge. Our calculations show that for typical superlattice parameters characteristic times for switching from a zero voltage state to a finite dc voltage state lie in the picosecond range.

We wish to thank the Deutscher Akademischer Austauschdienst (DAAD), the Bayerische Forschungsstiftung through the Bayerischer Forschungsverbund Hochtemperatur-Supraleiter (FORSUPRA), and the International Science Foundation (Grant N R8D000) for financial support.

References

1. Bloch, F.: Z. Physik **52**, 555 (1928).
2. Zener, C.: Proc. Roy. Soc. London Ser. A **145**, 523 (1934).
3. Esaki, L., Tsu, R.: IBM J. Res. Develop. **14**, 61 (1970); Raphael Tsu, in "Semiconductor interfaces, microstructures and devices: Properties and applications", edited by Z.C. Feng (Institute of Physics Publishing, Bristol and Philadelphia, 1993), p. 3
4. Sibille, A., Palmier, J.F., Wang, H., Mollot, F.: Phys. Rev. Lett. **64**, 52 (1990)
5. Beltram, F., Capasso, F., Sivco, D.L., Hutchinson, A.L., Chu, S.N.G., Cho, A.Y.: Phys. Rev. Lett. **64**, 3167 (1990)
6. Grahn, H.T., von Klitzing, K., Ploog, K., Döhler, G.H.: Phys. Rev. B **43**, 12094 (1991)
7. Sibille, A., Palmier, J.F., Minot, C.: in "Semiconductor interfaces and microstructures", edited by Z.C. Feng (World Scientific, Singapore, 1992), p. 31
8. Feldmann, J., Leo, K., Shah, J., Miller, D.A.B., Cunningham, J.E., Meier, T., von Plessen, G., Schulze, A., Thomas, P., Schmitt-Rink, S.: Phys. Rev. B **46**, 7252 (1992)
9. Waschke, C., Roskos, H.G., Schwedler, R., Leo, K., Kurz, H., Köhler, K.: Phys. Rev. Lett. **70**, 3319 (1993)
10. Ignatov, A.A., Schomburg, E., Renk, K.F., Schatz, W., Palmier, J.F., Mollot, F.: Annalen der Physik **3**, 137 (1994)
11. Ignatov, A.A., Renk, K.F., Dodin, E.P.: Phys. Rev. Lett. **70**, 1996 (1993)
12. Dunlap, D.H., Kovanis, V., Duncan, R.V., Simmons, J.: Phys. Rev. B **48**, 7975 (1993)
13. Ignatov, A.A., Romanov, Yu.A.: Radiophysics and Quantum Electronics (Consultants Bureau, New York) **21**, 91 (1978)
14. Ignatov, A.A., Shashkin, V.I.: Phys. stat. sol. (b) **110**, K117 (1982)
15. Ignatov, A.A., Romanov, Yu.A.: Phys. stat. sol. (b) **73**, 327 (1976)
16. Dunlap, D.H., Kenkre, Y.M.: Phys. Rev. B **34**, 3625 (1986); ibid. **37**, 6622 (1987)
17. Dunlap, D.H., Kenkre, V.M.: Phys. Lett. A **127**, 438 (1988)
18. Holthaus, M.: Phys. Rev. Lett. **69**, 351 (1992)
19. Zhao, X.-G.: Phys. Lett. A **167**, 291 (1992); X.-G. Zhao and Q. Niu, Phys. Lett. **A 191**, 181 (1994)
20. Wang, X.H., Yao, X.X.: Phys. Lett. A **167**, 295 (1992)
21. Hone, D.W., Holthaus, M. Phys. Rev. B **48**, 15123 (1993)
22. Zak, J.: Phys. Rev. Lett. **71**, 2623 (1993)
23. Barone, A., Paterno, G.: Physics and Applications of the Josephson Effect (Wiley, New York, 1982), Chap. 6

24. Kleiner, R., Steinmeyer, F., Kunkel, G., Müller, P.: Phys. Rev. Lett. **68**, 2394 (1992)
25. Ignatov, A.A., Dodin, E.P., Shashkin, V.I.: Mod. Phys. Lett. **B 5**, 1087 (1991)
26. Hadjazi, M., Palmier, J.F., Sibille, A., Wang, H., Paris, E., Mollot, F.: Electr. Lett. **29**, 648 (1993)
27. Minot, C., Le Person, H., Palmier, J.F., Sahri, N., Mollot, F., Planel, R.: Semicond. Sci. Technol. **9**, 789 (1994)
28. Prengel, F., Wacker, A., Schöll, E.: Phys. Rev. B **50**, 1705 (1994)
29. Grahn, H.T., Haug, R.J., Müller, W., Ploog, K.: Phys. Rev. Lett. **67**, 1618 (1991)
30. Grahn, H.T.: Phys. Scr. T **49**, 507 (1993)
31. Tsu, R., Esaki, L.: Phys. Rev. B **43**, 5204 (1991)
32. Meier, T., von Plessen, G., Thomas, P., Koch, S.W. Phys. Rev. Lett. **73**, 902 (1994)